

Interaction potentials and transport properties of Ba, Ba⁺, and Ba²⁺ in rare gases from He to Xe

Alexei A. Buchachenko, and Larry A. Viehland

Citation: *J. Chem. Phys.* **148**, 154304 (2018); doi: 10.1063/1.5025861

View online: <https://doi.org/10.1063/1.5025861>

View Table of Contents: <http://aip.scitation.org/toc/jcp/148/15>

Published by the [American Institute of Physics](#)

Articles you may be interested in

[Communication: Photoionization of degenerate orbitals for randomly oriented molecules: The effect of time-reversal symmetry on recoil-ion momentum angular distributions](#)

The Journal of Chemical Physics **148**, 151101 (2018); 10.1063/1.5026181

[Helium-induced electronic transitions in photo-excited Ba⁺-He_n exciplexes](#)

The Journal of Chemical Physics **148**, 144302 (2018); 10.1063/1.5022863

[Observation of photoassociation of ultracold sodium and cesium at the asymptote Na \(3S_{1/2}\) + Cs \(6P_{1/2}\)](#)

The Journal of Chemical Physics **148**, 174304 (2018); 10.1063/1.5023330

[Electrode redox reactions with polarizable molecules](#)

The Journal of Chemical Physics **148**, 154501 (2018); 10.1063/1.5022709

[Chemical waves in the O₂ + H₂ reaction on a Rh\(111\) surface alloyed with nickel. II. Photoelectron spectroscopy and microscopy](#)

The Journal of Chemical Physics **148**, 154705 (2018); 10.1063/1.5020381

[Chemical waves in the O₂ + H₂ reaction on a Rh\(111\) surface alloyed with nickel. I. Photoelectron emission microscopy](#)

The Journal of Chemical Physics **148**, 154704 (2018); 10.1063/1.5020372

PHYSICS TODAY

WHITEPAPERS

ADVANCED LIGHT CURE ADHESIVES

Take a closer look at what these environmentally friendly adhesive systems can do

READ NOW

PRESENTED BY
 MASTERBOND[®]
ADHESIVES | SEALANTS | COATINGS

Interaction potentials and transport properties of Ba, Ba⁺, and Ba²⁺ in rare gases from He to Xe

Alexei A. Buchachenko^{1,a)} and Larry A. Viehland^{2,b)}

¹Skolkovo Institute of Science and Technology, Skolkovo Innovation Center, Building 3, Moscow 143026, Russia

²Science Department, Chatham University, Pittsburgh, Pennsylvania 15232, USA

(Received 14 February 2018; accepted 3 April 2018; published online 19 April 2018)

A highly accurate, consistent set of *ab initio* interaction potentials is obtained for the title systems at the coupled cluster with singles, doubles, and non-iterative triples level of theory with extrapolation to the complete basis set limit. These potentials are shown to be more reliable than the previous potentials based on their long-range behavior, equilibrium properties, collision cross sections, and transport properties. *Published by AIP Publishing.* <https://doi.org/10.1063/1.5025861>

I. INTRODUCTION

Interatomic interactions of Ba and its cations with rare gases (RGs) are of interest for many fundamental and practical applications. Perhaps the hottest one is related to the search for the neutrino-less decay, $^{136}\text{Xe} \rightarrow ^{136}\text{Ba}^{2+} + 2e^{-}$, whose discovery may shed light on the nature of the neutrino. Ongoing experiments on EXO-200¹ and larger scale nEXO facilities need Ba detection schemes at the level of single-atom sensitivity, with one of the proposals relying on spectroscopy in a frozen Xe cryoprobe.² This search has revitalized the interest in Ba matrix isolation spectroscopy:³ two recent experimental studies with laboratory Ba sources showed complexities in the spectroscopy of neutrals and no evidence for cationic species.^{2,4}

In quite different contexts, excitation of Ba was used as a marker for solvation effects in a series of papers on Ar clusters^{5–9} as well as in studies with liquid He.^{10,11} Interactions with a single RG atom were probed through collision-induced absorption measurements^{12–16} and the spectroscopy of BaAr dimers, both neutral¹⁷ and ionized.¹⁸ Inelastic collision-induced processes were also investigated,^{19–23} providing the grounds for understanding non-radiative decay pathways in Ba emission spectroscopy with matrix isolation. Finally, Ba⁺ is an important astrophysical marker²⁴ for chemically peculiar stars,^{25,26} where one of the mechanisms controlling observed element (and isotope) abundances implies light-induced drift.^{27,28}

The transport properties of Ba and its cations with the RGs have been the subject of several studies. Gas-phase diffusion cross sections of neutral Ba in RGs have been measured for the ground and metastable states^{22,29,30} and used in modeling low-pressure discharges³¹ and Ba (emitter material) transport and radiation in fluorescence lamps.³² Cation transport properties have been studied as a function of E/n_0 , the ratio of the electrostatic field strength to the gas number density, in drift

tubes filled with He and Ar buffer gases.^{33–36} Momentum-transfer collisions are the primary determinants for the cooling of trapped ions, so one can use them to investigate cooling Ba⁺ with He and Ar coolants.³⁷ In addition to gas-phase studies, the mobility of Ba⁺ has been studied in superfluid He³⁸ and liquid Xe.³⁹

Studies of the doubly charged barium cations are not as numerous. Selected ion flow tube-tandem mass spectrometry combined with electrospray ionization gave evidence for formation of the RGBa^{2+} and $\text{RG}_2\text{Ba}^{2+}$ species by room-temperature termolecular association in He buffer gas.⁴⁰ Subsequently, complexes of Ba²⁺ and light alkaline-earth ions with Ar have been observed in inductively coupled plasma mass spectrometry.⁴¹

The above examples give rich and diverse information for theoretical analysis of, for example, the non-additive many-body effects in the spectra and transport of ions and neutrals.^{42–44} Vice versa, existing data provide good references for testing interaction and dynamical models.

The interaction potentials for Ba, Ba⁺, and Ba²⁺ with RG atoms were the subject of several theoretical studies, including semiempirical and *ab initio* ones.^{4,13,45–51} Particular attention has been given to the ground state interactions. McGuirk *et al.*⁵⁰ performed a systematic study of the Ba⁺- and Ba²⁺-RG potentials for RG from He to Rn at the coupled cluster level of *ab initio* theory, accounting for singles, doubles, and non-iterative triples, CCSD(T). For Ba ions, they used a 46-electron effective core potential (ECP) optimized at the Dirac-Fock level⁵² (ECP46MDF), with the specially constructed basis roughly equivalent to augmented, correlation-consistent, polarized valence set of quintuple-zeta quality, aug-cc-pV5Z.⁵³ With these potentials, comprehensive sets of gaseous ion transport coefficients, including mobilities and ion temperatures parallel and perpendicular to the field, were computed; they are available from an on-line database.⁵⁴ It was found that, in contrast to the temperatures of the drifting ion, the calculated mobilities of Ba⁺ in He and Ar deviate from the measured ones. Good agreement with the spectroscopic data¹⁸ on the Ba⁺-Ar complex was obtained. Later, the pseudopotential approach with core-polarization potentials was applied to

^{a)}a.buchachenko@skoltech.ru

^{b)}viehland@chatham.edu

Ba⁺-Xe and Ba-Xe complexes (one and two explicit electrons, respectively) to study⁵¹ several excited states (up to 6s → 9s excitation of Ba). The ground-state equilibrium distance and the well depth were found in these studies to be 3% longer and 25% larger than those reported by McGuirk *et al.*⁵⁰ Some new data on the Ba²⁺-RG complexes have recently emerged.⁴⁰⁻⁴²

The studies by Czuchaj *et al.*^{46,47,49} provide the most comprehensive description of Ba-RG neutrals to date and have been used quite extensively.^{7,8,10,30,55} These authors used the pseudopotential approach to combine two-electron Ba and eight (valence) electron RG descriptions. Remarkable deviations can be seen for the lowest states of Ba-Xe from the two-electron pseudopotential calculations.⁵¹ Finally, Davis and McCaffrey⁴ have employed the CCSD(T) method in conjunction with the ECP46MDF Ba effective-core potential⁵² and a corresponding aug-cc-pVQZ basis set⁵³ to calculate interaction potentials with Ar, Kr, and Xe.

The purpose of the present paper is to report on a comprehensive *ab initio* study of the ground-state potentials for Ba, Ba⁺, and Ba²⁺ interacting with the rare gases from He to Xe. First, we consider neutrals and cations at the CCSD(T) level of theory using a small core (SC) ECP⁵² and, in part, all-electron (AE) descriptions. We analyze different extents of correlation and address basis set superposition error, extrapolating to the complete basis set (CBS) limit. Second, we update the comparisons with existing experimental and theoretical data on the long-range and equilibrium properties of the neutral and charged Ba-RG complexes. Third, we use our best potentials in calculations of the transport cross sections and coefficients, including ion mobilities, temperatures, and diffusion coefficients, as well as neutral Ba diffusion coefficients.

In Sec. II, we describe the *ab initio* approaches, then follow systematic comparisons of the *ab initio* results at long range, through leading van der Waals coefficients, and near equilibrium, through equilibrium distances and well depths. These justify the approaches chosen for the global interaction potential calculations. The global potentials are compared with the available literature data and used for transport property calculations as described in Secs. III and IV for neutrals and ions, respectively. Conclusions follow in Sec. V.

II. AB INITIO CALCULATIONS

A. Methods

All calculations were performed using the methods implemented in the MOLPRO (ver. 2015.1) package.⁵⁶ In all diatomic calculations, the partially spin-restricted CCSD(T) method⁵⁷ was employed with a restricted Hartree-Fock reference. Counterpoise correction (CP) was included to overcome basis set superposition errors.⁵⁸

Our first calculations relied on the ECP description of Ba. The 46-electron ECP46MDF⁵² was employed together with augmented, correlation-consistent polarized core-valence basis sets, aug-cc-pwCVnZ, with $n = Q, T, 5$,⁵³ abbreviated as CnZ. All electrons were always correlated. These were combined with the following options for RG atoms with consistent basis set cardinal number n : He aug-cc-pVnZ,⁵⁹ Ne aug-cc-pCVnZ,⁶⁰ 1s² shell in core or correlated within

small-core (SC) option; Ar aug-cc-pwCVnZ,⁶¹ 1s²2s²2p⁶ or 1s² shells in core, in normal or SC runs, respectively. For Kr and Xe, effective core potentials ECP10MDF and ECP28MDF⁶² were employed with the aug-cc-pwCVnZ sets,⁶³ normally, the outer s^2p^6 shells were correlated, while in the SC option the preceding d^{10} shell was also included in the correlation treatment. Bond functions (BFs), if added, were placed at the midpoint of Ba-RG distance, R , using the 3s3p2d2f1g set.⁶⁴ Combined acronyms, e.g., ECP/CTZ or ECP/C5Z/SC/BF, fully define the computational scheme for all Ba-RG species.

The second set of calculations for He, Ne, and Ar explored the consequences of using an all-electron (AE) description of Ba with the relativistic atomic natural orbitals with core correlation (ANO-RCC) basis set.⁶⁵ It was supplemented by the set of spdfg diffuse primitives with exponents obtained as an even-tempered continuation of the two smallest exponents in the standard basis. Test calculations of atomic properties revealed negligible changes upon adding the second diffuse set. These tests also indicated that although an ANO-RCC basis was constructed for the third-order Douglas-Kroll-Hess scalar relativistic Hamiltonian,⁶⁶ the fourth-order approximation gives slightly better results. Normally, 46 inner Ba electrons were kept in the core, as in the ECP calculations, while within the small core (SC) option, a 28-electron core was used with the 4s²4p⁶4d¹⁰ shells correlated explicitly. This description was combined with the aug-cc-pV5Z basis for He,⁵⁹ aug-cc-pCV5Z-DK for Ne, and aug-cc-pwCV5Z-DK for Ar.⁶⁷ Regardless of the choice for the Ba core, the 2s²2p⁶ shells were correlated in Ne. For Ar, the 3s²3p⁶ and 2p⁶3s²3p⁶ shells were correlated normally and within the SC option, respectively. A 3s3p2d2f1g set of bond functions was added as described above. Combined acronyms, e.g., AE or AE/SC/BF, fully define the particular AE scheme.

Equivalent schemes were used for atomic properties, ionization potentials, and static and dynamic polarizabilities. The dipole and quadrupole static polarizabilities were calculated by means of the finite-field approach.^{68,69} The dynamic dipole polarizabilities of the neutral Ba and RG atoms were calculated using a third-order polarization propagator at the CCSD level, CCSD(3),^{70,71} as implemented through the equation-of-motion CCSD unit in MOLPRO.

ECP series are regular with respect to cardinal number n , thus allowing for extrapolation to the complete basis set (CBS) limit using $n = T, Q, 5$. For this purpose, we used the mixed exponential-Gaussian function^{72,73}

$$E(n) = E_{CBS} + B \exp[-(n-1)] + C \exp[-(n-1)^2], \quad (1)$$

where $E(n)$ is the electronic energy computed at the point (the distance for diatomic calculations or the field strength for finite-field calculations) with the basis cardinal number n and E_{CBS} is its extrapolated value. For testing purpose, the formula by Martin^{74,75}

$$E(n) = E_{CBS} + \frac{B}{\left(n + \frac{1}{2}\right)^4} + \frac{C}{\left(n + \frac{1}{2}\right)^6} \quad (2)$$

was also tried. Both equations have the advantage of linear extrapolation parameters, which makes them compatible with

the CP correction.⁷⁶ However, it was found that Eq. (2) is less reliable for atomic properties and is not trustworthy when the energy varies irregularly with n (see below). Hence, only the formula (1) is used in what follows.

B. Atomic properties and long-range coefficients

Our results for the first and second Ba ionization potentials, IP_1 and IP_2 , static dipole, $\alpha_D(0)$, and quadrupole, $\alpha_Q(0)$, polarizabilities of Ba, Ba^+ , and Ba^{2+} are presented in Table I. Here and hereafter, polarizabilities are given in atomic units, a_0^3 and a_0^5 , for $\alpha_D(0)$ and $\alpha_Q(0)$, respectively. The uncertainties indicated in Table I originate solely from the quality of the quadratic fits to energy-field dependences. The “other theory” entry presents literature results obtained with methods like ours or that have been recommended by other authors; the coverage is not exhaustive.

The results for the ionization potentials attest the relative accuracy of the treatment of systems containing Ba in different charge states. All *ab initio* results are lower than the experimental data;⁷⁷ the ECP/ CnZ series regularly approach the experimental values from below, ending up with an error of 0.25% at the CBS limit. The AE results are close to the ECP/CTZ ones. However, our AE/SC calculations indicate that explicit correlation of the Ba $4s^2 4p^6 4d^{10}$ electrons, not accounted for in the Dirac-Fock based ECP, further increases the ionization potential and may well compensate for about two-thirds of the remaining discrepancy at the CBS limit.

The $\alpha_D(0)$ of the neutral Ba was measured,⁷⁸ though with quite large error bars. Several theoretical calculations have also been reported. The result of CCSD(T) calculations by

Schäfer *et al.*⁷⁹ (275.5 a.u.) falls between our ECP/CTZ and ECP/CQZ values. The result from relativistic CCSDT (full correction to triples) is 273.9;⁸⁰ it should be superior to our AE/SC value. Other estimates at the relativistic coupled cluster level are 275.5 a.u.⁸¹ and 278.2 and 274.7 a.u.,⁸² giving in average 275 ± 3 a.u. Porsev and Derevianko⁸³ used relativistic configuration interaction plus many-body perturbation theory (CI+MBPT) to give the value of 272.1 a.u. and recommended that one use 273.5 ± 2 a.u. Our best ECP/CBS value falls within the quoted error bars, while our AE results are a bit higher; as with the ionization potentials, this indicates that there is a non-negligible effect of Ba $n = 4$ shell correlation. The $\alpha_Q(0)$ of the neutral agree well with the only available CI+MBPT value.⁸³

Two available measurements of $\alpha_D(0)$ for Ba^+ cations^{84,85} do not agree with each other within the combined error bars, even though they differ by 1% only. Table I features the results of the relativistic coupled cluster calculations;^{80,86} coupled cluster⁸⁷ (124.15 a.u.) and relativistic MBPT⁸⁸ (124.51 a.u.) values should also be mentioned. The best present ECP/CBS value looks too high (by 0.5% with respect to experiment⁸⁵), whereas AE calculations once again indicate a non-negligible effect of the $n = 4$ shells' correlation. Measured quadrupole polarizabilities^{84,85,89} disagree with each other by surprising amounts. Other theoretical studies^{87,88,90} strongly support the value in Ref. 85 and discuss the reason for the differences. Our results are similar, with ECP/CBS and AE/SC estimates closer to upper and lower experimental bounds,⁸⁵ respectively.

The static dipole polarizability value of Ba^{2+} (10.17 a.u.) was used for parameterization of two-electron pseudopotentials.^{49,91} The most reliable theoretical value (10.53 a.u.) was

TABLE I. First and second ionization potentials of Ba atom (cm^{-1}) and static dipole and quadrupole polarizabilities of Ba atom and cations (a.u.). Uncertainties of the large digit(s) are given in parentheses.

| Scheme | Ba | | Ba^+ | | | Ba^{2+} | | |
|--------------|----------------------|------------------------|------------------------|------------------------|------------------------|------------------------|----------------------|---------------------|
| | $\alpha_D(0)^a$ | $\alpha_Q(0)$ | IP_1 | $\alpha_D(0)$ | $\alpha_Q(0)$ | IP_2 | $\alpha_D(0)$ | $\alpha_Q(0)$ |
| ECP/CTZ | 276.19/269.82 | 8600 | 41 751.3 | 125.52 | 3780 | 121 988.3 | 10.59 | 45.1 |
| ECP/CQZ | 274.44/268.28 | 8800 | 41 892.6 | 124.12 | 4170 | 122 352.2 | 10.63 | 46.2 |
| ECP/C5Z | 274.74/268.39 | 8900 | 41 915.8 | 124.33 | 4460 | 122 394.1 | 10.60 | 45.9 |
| ECP/CBS | 274.92/268.39 | 8950 | 41 929.0 | 124.46 | 4630 | 122 417.5 | 10.58 | 45.7 |
| AE | 277.56/272.44 | 9300 | 41 763.1 | 125.66 | 4360 | 121 964.4 | 10.66 | 45.7 |
| AE/SC | 276.45/270.81 | 9100 | 41 831.2 | 124.48 | 4125 | 122 187.3 | 10.59 | 45.4 |
| Uncertainty | ± 0.01 | ± 25 | | ± 0.01 | ± 10 | | ± 0.01 | ± 0.1 |
| Experiment | 268(22) ^b | | 42 034.91 ^c | 125.5(10) ^d | 2050(100) ^d | 122 721.2 ^c | 10.3(2) ^e | 51(10) ^e |
| Other theory | 275.5 ^g | 8900(650) ^h | | 123.88(5) ^f | 4420(250) ^f | | | |
| | 273.9 ⁱ | | 123.07 ^j | 4092 ^j | 10.53 ⁱ | | | |
| | | | | 124.40 ^k | 4270(27) ^l | | | |

^aCCSD(T) finite-field/CCSD(3) zero-frequency values are given for the present work.

^bReference 78.

^cReference 77.

^dReference 84.

^eReference 92.

^fReference 85.

^gReference 79.

^hReference 83.

ⁱReference 80.

^jReference 88.

^kReference 86.

^lReference 90.

given by Lim and Schwerdtfeger,⁸⁰ who also referred to earlier estimates ranging from 10 to 11.7 a.u., while the only experimental values were obtained from the Ba⁺ Rydberg series.⁹² Our values corroborate the literature data.

It is concluded that the description used here, at the level of ECP/C5Z or ECP/CBS, reproduces atomic ionization potentials and polarizability data within 1%. The AE description performs nearly at the level of the ECP/CTZ scheme, but consistently reveals non-negligible correlation effects of the 4s²4p⁶4d¹⁰ Ba shells.

The lowest-order long-range interaction of neutral Ba with RG atoms is determined by the dispersion coefficient

$$C_6 = \frac{3}{\pi} \int_0^\infty \alpha_D(i\omega) \alpha_D^{\text{RG}}(i\omega) d\omega, \quad (3)$$

which is related to the dynamic dipole polarizabilities of both atoms.⁹³ The latter quantities were computed using the CCSD(3) polarization propagator approach. Table I, which presents zero-frequency results for Ba atom, shows that this approach systematically underestimates the CCSD(T) finite-field values by 2%. Similar underestimation was found for the RG atoms except He, for which both approaches agree up to the fourth significant digit. This suggests that the discrepancy primarily originates from the non-iterative triple correction accounted for in the finite-field calculations. Indeed, CCSD finite field results for the heavier RG atoms are in much better (although not complete) agreement with the polarization propagator calculations. Dispersion coefficients C_6 , as well as static dipole polarizabilities of RG atoms, are discussed below in comparison with the coefficients deduced by fitting

TABLE II. Equilibrium distances R_e (Å) and well depths D_e (cm⁻¹) of the Ba^{0,+2+}-RG complexes from the CCSD(T) calculations.

| Scheme | He | | Ne | | Ar | | Kr | | Xe | |
|------------------|-------|--------|-------|---------|-------|---------|-------|---------|-------|---------|
| | R_e | D_e | R_e | D_e | R_e | D_e | R_e | D_e | R_e | D_e |
| Ba | | | | | | | | | | |
| ECP/CTZ | 6.831 | 2.12 | 6.098 | 7.68 | 5.670 | 47.27 | 5.563 | 77.81 | 5.644 | 112.84 |
| ECP/CQZ | 6.722 | 2.41 | 5.934 | 10.00 | 5.549 | 56.26 | 5.449 | 92.12 | 5.507 | 133.63 |
| ECP/C5Z | 6.670 | 2.56 | 5.853 | 11.22 | 5.506 | 60.37 | 5.407 | 97.88 | 5.465 | 142.49 |
| ECP/CTZ/BF | 6.689 | 2.51 | 5.869 | 10.60 | 5.512 | 60.03 | 5.413 | 97.49 | 5.461 | 142.96 |
| ECP/CQZ/BF | 6.652 | 2.61 | 5.834 | 11.60 | 5.488 | 62.06 | 5.394 | 101.23 | 5.454 | 145.62 |
| ECP/CV5Z/BF | 6.645 | 2.66 | 5.810 | 12.01 | 5.479 | 63.06 | 5.387 | 101.43 | 5.451 | 147.42 |
| ECP/CBS | 6.647 | 2.64 | 5.816 | 11.97 | 5.476 | 62.90 | 5.381 | 101.37 | 5.447 | 147.95 |
| ECP/BF/CBS | 6.637 | 2.69 | 5.795 | 12.25 | 5.474 | 63.65 | 5.383 | 102.14 | 5.448 | 148.47 |
| ECP/C5Z/SC | ... | ... | 5.855 | 11.16 | 5.503 | 60.41 | 5.393 | 98.37 | 5.446 | 146.65 |
| AE/BF | 6.667 | 2.60 | 5.826 | 11.86 | 5.479 | 63.22 | ... | ... | ... | ... |
| AE/BF/SC | 6.654 | 2.63 | 5.813 | 12.00 | 5.463 | 63.97 | ... | ... | ... | ... |
| Ba ⁺ | | | | | | | | | | |
| ECP/CTZ | 4.992 | 20.61 | 4.391 | 59.17 | 3.526 | 534.00 | 3.574 | 885.23 | 3.747 | 1323.88 |
| ECP/CQZ | 4.950 | 21.77 | 4.292 | 72.63 | 3.396 | 658.02 | 3.481 | 1059.79 | 3.660 | 1528.27 |
| ECP/C5Z | 4.933 | 22.15 | 4.279 | 74.14 | 3.361 | 724.59 | 3.457 | 1131.15 | 3.633 | 1616.31 |
| ECP/CTZ/BF | 4.948 | 21.91 | 4.330 | 66.38 | 3.375 | 717.76 | 3.465 | 1150.85 | 3.645 | 1682.95 |
| ECP/CQZ/BF | 4.922 | 22.47 | 4.268 | 73.93 | 3.359 | 733.56 | 3.455 | 1146.69 | 3.630 | 1647.90 |
| ECP/C5Z/BF | 4.917 | 22.64 | 4.246 | 76.45 | 3.348 | 751.45 | 3.446 | 1163.80 | 3.621 | 1662.70 |
| ECP/CBS | 4.927 | 22.38 | 4.260 | 75.03 | 3.341 | 765.74 | 3.440 | 1174.98 | 3.608 | 1671.88 |
| ECP/BF/CBS | 4.911 | 22.73 | 4.236 | 77.94 | 3.344 | 762.15 | 3.439 | 1171.44 | 3.613 | 1671.53 |
| ECP/C5Z/SC | ... | ... | 4.277 | 73.75 | 3.354 | 724.14 | 3.447 | 1127.63 | 3.619 | 1619.17 |
| AE/BF | 4.937 | 22.28 | 4.258 | 75.61 | 3.361 | 729.42 | ... | ... | ... | ... |
| AE/BF/SC | 4.923 | 22.55 | 4.249 | 76.67 | 3.365 | 721.06 | ... | ... | ... | ... |
| Ba ²⁺ | | | | | | | | | | |
| ECP/CTZ | 2.860 | 604.74 | 2.939 | 1088.69 | 3.165 | 3302.41 | 3.267 | 4425.85 | 3.450 | 6001.58 |
| ECP/CQZ | 2.847 | 633.37 | 2.909 | 1147.01 | 3.128 | 3502.15 | 3.248 | 4670.42 | 3.414 | 6289.87 |
| ECP/C5Z | 2.838 | 645.34 | 2.887 | 1183.75 | 3.122 | 3572.39 | 3.235 | 4748.39 | 3.402 | 6400.45 |
| ECP/CTZ/BF | 2.843 | 643.86 | 2.893 | 1166.86 | 3.123 | 3642.48 | 3.238 | 4861.60 | 3.402 | 6604.39 |
| ECP/CQZ/BF | 2.837 | 649.28 | 2.897 | 1192.75 | 3.119 | 3609.49 | 3.232 | 4801.70 | 3.400 | 6485.84 |
| ECP/C5Z/BF | 2.833 | 651.88 | 2.893 | 1201.92 | 3.116 | 3612.09 | 3.229 | 4798.57 | 3.397 | 6472.58 |
| ECP/CBS | 2.832 | 652.45 | 2.877 | 1206.26 | 3.116 | 3614.00 | 3.227 | 4794.72 | 3.387 | 6466.90 |
| ECP/BF/CBS | 2.832 | 653.05 | 2.880 | 1208.18 | 3.115 | 3613.88 | 3.227 | 4796.24 | 3.388 | 6466.15 |
| ECP/C5Z/SC | ... | ... | 2.887 | 1180.96 | 3.120 | 3565.80 | 3.230 | 4714.70 | 3.393 | 6355.21 |
| AE/BF | 2.844 | 644.25 | 2.891 | 1190.75 | 3.126 | 3575.82 | ... | ... | ... | ... |
| AE/BF/SC | 2.838 | 651.22 | 2.885 | 1205.04 | 3.120 | 3599.18 | ... | ... | ... | ... |

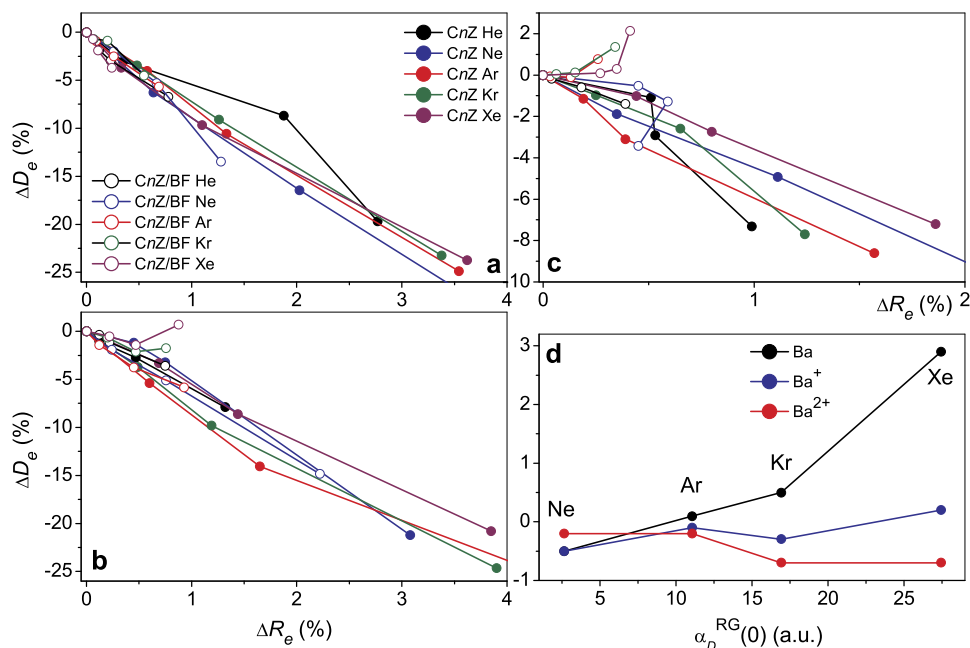


FIG. 1. Panels [(a)–(c)]: Convergence of R_e and D_e values to the CBS limit along the ECP/ CnZ and ECP/ CnZ/BF sequences for Ba-RG (a), Ba^+ -RG (b), and Ba^{2+} -RG (c) complexes. Panel (d): Effect of RG subvalence correlation on D_e of the $Ba^{0,+2+}$ -RG complexes shown as the percentage deviation between the ECP/C5Z/SC and ECP/C5Z results.

the diatomic interaction potentials. These quantities determine the long range coefficients for Ba cations ($C_4 = \alpha_D^{RG}(0)/2$) and dications ($C_4 = 2\alpha_D^{RG}(0)$).

C. Equilibrium properties

To analyze the convergence of our *ab initio* results for the equilibrium distance, R_e , and the binding energy, D_e , of the complexes, short radial grids covering the potential well regions were used, the same for each of the Ba^{n+} -RG ($n = 0-2$) species in all calculations. Five-point spline interpolations with quadratic derivatives at the endpoints were used to find the potential minima. The results are presented in Table II. It should be noted that R_e and D_e are given with 3 and 2 decimal digits, respectively, to better emphasize the small differences; the interpolation procedure may introduce larger uncertainties.

It is useful to consider first the CBS limit attainable with ECP calculations through two sequences, with and without bond functions. Generally, the two limiting values differ marginally, i.e., only to an extent comparable with the ambiguities of the extrapolating function and potential interpolation. The largest deviations can be seen in the Ba and Ba^+ complexes with He and Ne, where inclusion of the bond functions shrinks the bond length by 0.01-0.025 Å. The first three panels of Fig. 1 demonstrate the convergence of our ECP/ CnZ and ECP/ CnZ/BF results in terms of the relative percentage deviations of R_e and D_e from the limiting CBS values. Inclusion of bond functions always brings the results much closer to the limit, and normally the C5Z/BF calculations are accurate within 1%-2%. For the neutrals [panel (a)], both the CnZ and CnZ/BF series show a regular pattern: the interaction gets stronger with increasing n . For cations interacting with the heaviest Kr and Xe atoms [panel (b)], D_e at the CTZ/BF level

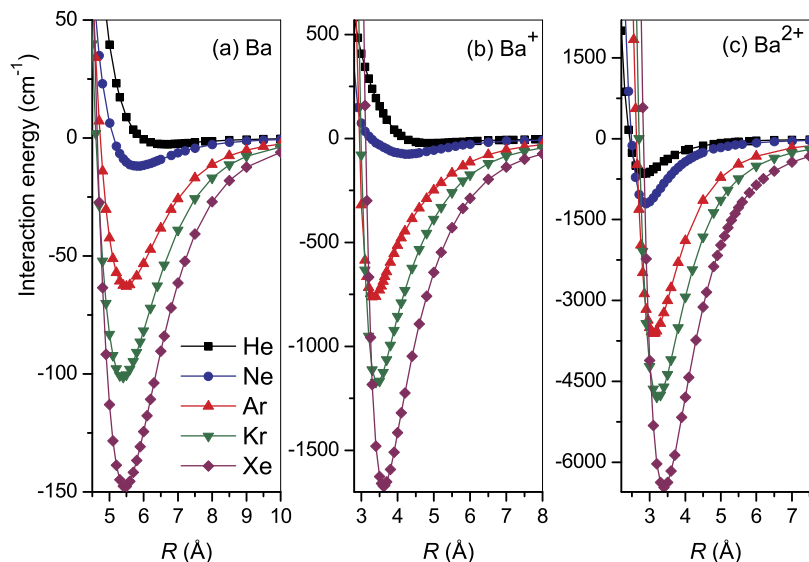


FIG. 2. ECP/CBS potentials of the Ba-RG (a), Ba^+ -RG (b), and Ba^{2+} -RG (c) complexes.

TABLE III. Parameters of the Ba-RG interaction potentials from the CCSD(T) ECP calculations and literature. σ and R_e in Å, C_6 in a.u., and D_e , D_0 , ω_e , $\omega_e x_e$, and B_0 in cm^{-1} . See text for additional explanations. For quantities obtained by fits, uncertainty of the last digit is given in parentheses if it exceeds one half of the digit presented.

| RG | Method/Ref. | σ | R_e | D_e | C_6 | $C_6(\text{as})$ | D_0 | ω_e | $\omega_e x_e$ | B_0 |
|--------------|--------------|----------|-------|-------|---------|------------------|-------|-------------------|------------------|----------|
| He | CTZ | 6.102 | 6.829 | 2.1 | 54.6(1) | 55.9 | 0.3 | 0.92 ^a | ... ^a | 0.06(1) |
| | CQZ | 6.003 | 6.721 | 2.4 | 54.7(1) | 55.9 | 0.4 | 1.02 | ... | 0.076(7) |
| | C5Z | 5.964 | 6.676 | 2.6 | 54.2(2) | 55.8 | 0.4 | 1.07 | ... | 0.076(1) |
| | CBS | 5.941 | 6.651 | 2.6 | 53.8(3) | ... | 0.4 | 1.10 | ... | 0.077(5) |
| | C5Z/BF | 5.933 | 6.642 | 2.7 | 55.8(1) | 55.8 | 0.5 | 1.11 | ... | 0.077(5) |
| | Reference 47 | | | 6.4 | 3.5 | | | | | |
| Reference 48 | | | 5.8 | 5 | | | | | | |
| Ne | CTZ | 5.395 | 6.106 | 7.7 | 100(1) | 102.9 | 5.3 | 5.2 | 0.90 | 0.0239 |
| | CQZ | 5.220 | 5.932 | 10.0 | 107 | 108.9 | 7.2 | 6.1 | 0.95 | 0.0256 |
| | C5Z | 5.153 | 5.857 | 11.2 | 109 | 110.5 | 8.2 | 6.5 | 0.97 | 0.0263 |
| | CBS | 5.115 | 5.815 | 12.0 | 109 | ... | 8.8 | 6.8 | 0.99 | 0.0267 |
| | C5Z/BF | 5.113 | 5.812 | 12.0 | 109 | 110.5 | 8.9 | 6.8 | 0.99 | 0.0268 |
| | Reference 49 | | | 5.3 | 64 | | | 22 | | |
| Ar | CTZ | 4.912 | 5.666 | 47.3 | 411 | 419.0 | 42.6 | 9.8 | 0.55(2) | 0.0166 |
| | CQZ | 4.803 | 5.552 | 56.2 | 418 | 423.7 | 51.1 | 10.7 | 0.53(1) | 0.0173 |
| | C5Z | 4.757 | 5.508 | 60.4 | 417 | 423.2 | 51.1 | 10.7 | 0.52 | 0.0176 |
| | CBS | 4.731 | 5.482 | 62.9 | 417 | – | 57.4 | 11.3 | 0.51 | 0.0178 |
| | C5Z/BF | 4.734 | 5.485 | 63.1 | 418(2) | 423.2 | 57.6 | 11.3 | 0.52 | 0.0177 |
| | Reference 49 | | | 5.6 | 73 | | | 16 | | |
| Reference 4 | | | 5.62 | 54.2 | | | | | | |
| Kr | CTZ | 4.791 | 5.569 | 77.8 | 613(4) | 630.7 | 73.2 | 9.3 | 0.27 | 0.0103 |
| | CQZ | 4.667 | 5.446 | 92.1 | 618(1) | 630.3 | 92.1 | 10.1 | 0.27 | 0.0108 |
| | C5Z | 4.628 | 5.408 | 97.9 | 618(1) | 630.8 | 92.7 | 10.5 | 0.27 | 0.0109 |
| | CBS | 4.606 | 5.387 | 101.4 | 618(1) | ... | 96.5 | 10.6 | 0.27 | 0.0110 |
| | C5Z/BF | 4.607 | 5.393 | 101.4 | 618(1) | 630.8 | 96.2 | 10.6 | 0.26 | 0.0110 |
| | Reference 49 | | | 5.7 | 80 | | | 13 | | |
| Reference 4 | | | 5.57 | 84.0 | | | | | | |
| Xe | CTZ | 4.834 | 5.641 | 112.8 | 969(2) | 988.4 | 108.1 | 9.5 | 0.19 | 0.0078 |
| | CQZ | 4.702 | 5.509 | 133.6 | 966(6) | 984.8 | 128.5 | 10.4 | 0.19 | 0.0082 |
| | C5Z | 4.661 | 5.471 | 142.6 | 965(2) | 986.4 | 137.2 | 10.8 | 0.19 | 0.0083 |
| | CBS | 4.638 | 5.450 | 147.9 | 965(6) | ... | 142.4 | 11.0 | 0.19 | 0.0084 |
| | C5Z/BF | 4.637 | 5.454 | 147.4 | 971(2) | 986.4 | 141.9 | 10.9 | 0.19 | 0.0083 |
| | Reference 49 | | | 5.9 | 101 | | | 11 | | |
| Reference 4 | | | 5.55 | 131.1 | | | | | | |
| Reference 51 | | | 4.56 | 499 | | | 22 | 0.815 | | |

^aFor Ba–He potentials supporting one vibrational level, a half of zero point energy ($D_e - D_0$) is given as ω_e and $\omega_e x_e$ cannot be determined.

is overestimated, while for Ba^{2+} -RG the CBS limit for D_e is regularly approached from above for Ar, Kr, and Xe [panel (c)]. Ba^{2+} -Ne presents the only case of irregular convergence in R_e . Such variations do not cause a problem for flexible Eq. (1), but are at odds with the common understanding⁹⁴ of the CBS extrapolation.

Correlation effects of the sub-valence electrons in RG atoms can be assessed by referring the C5Z/SC results to the C5Z ones. These look important only for the Kr and Xe systems, where they lead to bond shrinkage by at most 0.3%. The trends in D_e are depicted in panel (d) in Fig. 1. The binding energy increases for neutrals from Ar to Xe and for Ba^+ -Xe. None of the variations exceed 1% except for Ba–Xe, where the correlation of $4d^{10}$ electrons reduces the D_e value by 3%.

Our all-electron results agree with the ECP ones remarkably well. The binding energies of the neutrals are close to the CBS limits, although the bond lengths are slightly longer.

For the cations, the AE calculations are roughly on par with those at the ECP/CQZ/BF level, with Ba^{2+} -Ar a remarkable exception. These differences may reflect both basis set completeness and the way we account for the scalar relativistic effects. Correlation of $4s^2 4p^6 4d^{10}$ electrons in Ba that cannot be recovered with ECP produces nearly constant effects, decreasing the bond length by 0.2%-0.3% and increasing binding energy by 0.7%-1.4%. The exception is that the Ba^+ -Ar interaction becomes weaker.

Despite occasional deviations, the present calculations give a consistent picture of the variation of equilibrium properties with the Ba charge state, the nature of the RG atom, and the level of the *ab initio* approach. The “chemical” trends are in line with those discussed qualitatively by McGuirk *et al.*⁵⁰ In what follows, we will concentrate on the ECP/CBS and ECP/C5Z/BF schemes that are the best compromises between the expense and the accuracy of the global interaction potential calculations.

TABLE IV. Parameters of the Ba⁺-RG interaction potentials from the CCSD(T) ECP calculations and literature. σ and R_e in Å, C_4 in a.u., and D_e , D_0 , ω_e , $\omega_e x_e$, and B_0 in cm⁻¹. See also caption of Table III.

| RG | Method/Ref. | σ | R_e | D_e | C_4 | $C_4(\text{as})$ | D_0 | ω_e | $\omega_e x_e$ | B_0 |
|---------------------------|---------------------------|----------|---------|---------|----------|------------------|-----------|------------|----------------|---------|
| He | CTZ | 4.295 | 4.998 | 20.6 | 0.71 | 0.69 | 12.6 | 15.9 | 3.26 | 0.152 6 |
| | CQZ | 4.249 | 4.946 | 21.8 | 0.71 | 0.69 | 13.4 | 16.6 | 3.37 | 0.146 4 |
| | C5Z | 4.234 | 4.931 | 22.2 | 0.71 | 0.69 | 13.7 | 16.9 | 3.42 | 0.157 4 |
| | CBS | 4.225 | 4.921 | 22.4 | 0.71 | 0.69 | 13.8 | 17.0 | 3.45 | 0.158 1 |
| | C5Z/BF | 4.222 | 4.917 | 22.6 | 0.71 | 0.69 | 14.0 | 17.2 | 3.99 | 0.158 5 |
| | Reference 50 | | 4.950 | 21.8 | | | 13.4 | 16.7 | 3.39 | |
| Ne | CTZ | 3.586 | 4.397 | 59.0 | 1.24 | 1.23 | 52.3 | 14.8(2) | 1.16(4) | 0.048 5 |
| | CQZ | 3.416 | 4.296 | 72.6 | 1.33 | 1.32 | 65.2 | 16.0(1) | 1.04(1) | 0.051 2 |
| | C5Z | 3.328 | 4.278 | 74.1 | 1.36 | 1.34 | 66.8 | 15.7(1) | 0.96(3) | 0.051 7 |
| | CBS | 3.254 | 4.267 | 75.0 | 1.37 | 1.34 | 67.7 | 15.4(1) | 0.92(3) | 0.052 1 |
| | C5Z/BF | 3.264 | 4.246 | 76.5 | 1.36 | 1.34 | 69.1 | 15.6(1) | 0.90(3) | 0.052 6 |
| | Reference 50 | | 4.291 | 72.6 | | | 65.4 | 15.1 | 0.82 | |
| Ar | CTZ | 3.056 | 3.529 | 533.8 | 5.54 | 5.50 | 512.5 | 42.5(2) | 1.64(4) | 0.042 9 |
| | CQZ | 2.974 | 3.401 | 658.0 | 5.65 | 5.61 | 630.4 | 56.4 | 2.55(2) | 0.046 3 |
| | C5Z | 2.944 | 3.361 | 724.6 | 5.64 | 5.60 | 694.3 | 62.4 | 2.74(2) | 0.047 5 |
| | CBS | 2.927 | 3.339 | 765.8 | 5.63 | 5.60 | 734.0 | 65.6 | 2.80(2) | 0.048 1 |
| | C5Z/BF | 2.913 | 3.348 | 751.5 | 5.64 | 5.60 | 720.4 | 63.9 | 2.72(2) | 0.047 9 |
| | Reference 50 | | 3.385 | 693.1 | | | 664.3 | 58.6 | 2.19 | |
| | Reference 50 ^a | | 3.38(1) | 720(30) | | | | 59(1) | | |
| | Reference 45 ^b | | 3.47 | 800 | | | | | | |
| | Reference 41 ^c | | | 530 | | | | | | |
| Reference 18 ^d | | | 680 | | | | 61.7(1.5) | 2.3(0.2) | 0.048 08(2) | |
| Kr | CTZ | 3.099 | 3.584 | 884.7 | 8.58(1) | 8.57 | 862.6 | 44.4 | 0.97 | 0.024 9 |
| | CQZ | 3.031 | 3.491 | 1059.3 | 8.61 | 8.60 | 1033.2 | 52.6 | 1.09 | 0.026 3 |
| | C5Z | 3.004 | 3.457 | 1131.1 | 8.62 | 8.60 | 1103.5 | 55.9 | 1.13 | 0.026 8 |
| | CBS | 2.889 | 3.438 | 1175.4 | 8.62 | 8.60 | 1146.8 | 57.8 | 1.14 | 0.027 1 |
| | C5Z/BF | 2.994 | 3.446 | 1163.9 | 8.62(6) | 8.60 | 1135.7 | 56.9 | 1.12 | 0.027 0 |
| | Reference 50 | | 3.479 | 1093.0 | | | 1066.3 | 53.9 | 1.02 | |
| Xe | CTZ | 3.225 | 3.750 | 1322.5 | 13.94(1) | 13.98 | 1299.8 | 45.4 | 0.56 | 0.017 7 |
| | CQZ | 3.159 | 3.667 | 1526.8 | 13.94 | 13.98 | 1501.3 | 51.2 | 0.61 | 0.018 5 |
| | C5Z | 3.132 | 3.623 | 1616.7 | 13.95(1) | 13.97 | 1589.9 | 53.7 | 0.64 | 0.018 7 |
| | CBS | 3.116 | 3.612 | 1672.2 | 13.96(1) | 13.97 | 1644.6 | 55.3 | 0.65 | 0.019 1 |
| | C5Z/BF | 3.121 | 3.621 | 1662.7 | 13.95(1) | 13.97 | 1635.5 | 54.6 | 0.63 | 0.019 0 |
| | Reference 50 | | 3.653 | 1568.9 | | | 1542.9 | 52.3 | 0.61 | |
| Reference 51 | | 3.77 | 1971 | | | | 54 | 0.59 | | |

^a“Best values” from CCSD(T) calculations with extended basis set and correlation treatment.

^bInversion of the transport data using the (n , 6, 4) potential model.

^cDensity functional theory.

^dDerived from the BaAr⁺ spectroscopy.

D. Interaction potentials

The ECP/CBS interaction potentials computed on wide grids of interatomic distances are shown for neutral, singly, and doubly charged Ba-RG complexes in panels [(a)–(c)], respectively, of Fig. 2. To better guide the eye, the energy scale is enlarged in panels (b) and (c) by factors of approximately 11 and 44 with respect to panel (a). Tables III–V give the parameters of ECP/ C_n Z, ECP/CBS, and ECP/C5Z/BF potentials. The C_n coefficients were obtained by fitting the long-range portion of the computed potentials (4–7 points at distances exceeding 30 Å). Their asymptotic estimates, $C_n(\text{as})$, were obtained as described above. The distance, σ , at which the potential energy is equal to zero, and the values of R_e and D_e were obtained from spline interpolations among the *ab initio* points, with derivatives at the end points set according to the values of C_n . The D_0 values are the dissociation energies including the zero-point

energy; they were obtained by solving the nuclear Schrödinger equation for the ground vibrational level. The vibrational constants, ω_e and $\omega_e x_e$, were determined by a cubic-spline fit to the 10 (3 in the case of Ba–Ne) lowest vibrational levels computed in the same way. The rotational constants, B_0 , were deduced by quadratic fits to the dependence of the ground vibrational energy upon the rotational momentum, $J(J + 1)$, for $J < 10$ (2 or 3 in the case of Ba–He). In all nuclear calculations, the masses used were those of the most abundant isotope: ¹³⁸Ba, ⁴He, ²⁰Ne, ⁴⁰Ar, ⁸⁴Kr, and ¹³²Xe. Finally, the *ab initio* points are reproduced in the [supplementary material](#) for this paper.

The results in Table III confirm the conclusions given above for equilibrium properties. From CTZ to C5Z, and further to the CBS limit, the interaction strength increases, as manifested by decreasing σ and increasing vibrational and rotational constants. The C5Z/BF calculations provide

TABLE V. Same as Table IV but for Ba²⁺-RG interaction potentials.

| RG | Method/Ref. | σ | R_e | D_e | C_4 | $C_4(\text{as})$ | D_0 | ω_e | $\omega_e x_e$ | B_0 |
|--------------|--------------|----------|-------|--------|-------|------------------|--------|------------|----------------|--------|
| He | CTZ | 2.464 | 2.867 | 603.7 | 2.76 | 2.76 | 521.9 | 175.2(4) | 17.4(1) | 0.5055 |
| | CQZ | 2.445 | 2.844 | 633.6 | 2.77 | 2.77 | 548.7 | 182.5(5) | 18.0(1) | 0.5143 |
| | C5Z | 2.437 | 2.836 | 645.7 | 2.77 | 2.77 | 559.6 | 185.3(5) | 18.2(1) | 0.5177 |
| | CBS | 2.433 | 2.831 | 652.8 | 2.77 | 2.77 | 566.0 | 186.9 | 18.3(1) | 0.5197 |
| | C5Z/BF | 2.435 | 2.833 | 651.9 | 2.77 | 2.77 | 565.4 | 186.2(6) | 18.2(1) | 0.5187 |
| | Reference 50 | | 2.842 | 637.6 | | | 552 | 175.7 | 14.0 | |
| | Reference 46 | | 2.65 | 950 | | | | | | |
| Ne | CTZ | 2.528 | 2.937 | 1089.2 | 4.85 | 4.92 | 1036.4 | 107.3 | 3.27(1) | 0.1104 |
| | CQZ | 2.504 | 2.914 | 1147.4 | 5.20 | 5.26 | 1043.5 | 109.7 | 3.28(2) | 0.1122 |
| | C5Z | 2.491 | 2.897 | 1183.3 | 5.30 | 5.36 | 1127.8 | 113.0 | 3.36(2) | 0.1135 |
| | CBS | 2.484 | 2.887 | 1205.2 | 5.36 | 5.36 | 1148.7 | 114.9 | 3.40(2) | 0.1143 |
| | C5Z/BF | 2.487 | 2.893 | 1201.9 | 5.30 | 5.36 | 1146.0 | 113.6 | 3.31(1) | 0.1138 |
| | Reference 50 | | 2.902 | 1162.5 | | | 1108 | 110.9 | 3.15 | |
| | Reference 47 | | 2.67 | 1650 | | | | | | |
| Ar | CTZ | 2.670 | 3.164 | 3302.4 | 21.81 | 22.02 | 3244.2 | 116.6 | 1.18 | 0.0541 |
| | CQZ | 2.642 | 3.130 | 3501.4 | 21.24 | 22.44 | 3440.6 | 122.1 | 1.20 | 0.0553 |
| | C5Z | 2.631 | 3.120 | 3572.2 | 22.20 | 22.39 | 3510.7 | 123.4 | 1.19 | 0.0556 |
| | CBS | 2.625 | 3.114 | 3613.1 | 22.17 | 22.39 | 3552.1 | 124.1 | 1.19 | 0.0558 |
| | C5Z/BF | 2.627 | 3.116 | 3612.1 | 22.20 | 22.39 | 3550.3 | 123.9 | 1.18 | 0.0558 |
| | Reference 50 | | 3.130 | 3519.9 | | | 3459 | 122.1 | 1.19 | |
| | Reference 47 | | 3.12 | 3050 | | | | | | |
| Kr | CTZ | 2.744 | 3.275 | 4422.9 | 33.81 | 34.26 | 4374.3 | 97.1 | 0.59 | 0.0300 |
| | CQZ | 2.718 | 3.245 | 4670.5 | 33.94 | 34.39 | 4620.1 | 100.8 | 0.59 | 0.0306 |
| | C5Z | 2.707 | 3.233 | 4749.0 | 33.96 | 34.41 | 4698.1 | 101.8 | 0.59 | 0.0308 |
| | CBS | 2.700 | 3.226 | 4795.5 | 33.97 | 34.41 | 4744.3 | 102.4 | 0.59 | 0.0310 |
| | C5Z/BF | 2.702 | 3.229 | 4798.6 | 33.96 | 34.41 | 4747.4 | 102.3 | 0.59 | 0.0309 |
| | Reference 50 | | 3.244 | 4682.6 | | | 4632 | 100.8 | 0.59 | |
| | Reference 47 | | 3.28 | 3820 | | | | | | |
| Xe | CTZ | 2.864 | 3.448 | 6001.6 | 55.02 | 55.92 | 5955.9 | 90.7 | 0.38 | 0.0210 |
| | CQZ | 2.836 | 3.415 | 6290.6 | 55.01 | 55.92 | 6243.7 | 93.7 | 0.36 | 0.0214 |
| | C5Z | 2.824 | 3.402 | 6400.4 | 55.05 | 55.99 | 6352.9 | 94.9 | 0.37 | 0.0216 |
| | CBS | 2.818 | 3.394 | 6465.9 | 55.07 | 55.99 | 6418.0 | 95.6 | 0.37 | 0.0217 |
| | C5Z/BF | 2.819 | 3.397 | 6472.6 | 55.05 | 55.99 | 6424.9 | 95.3 | 0.36 | 0.0216 |
| | Reference 50 | | 3.413 | 6309.2 | | | 6262 | 94.0 | 0.37 | |
| | Reference 47 | | 3.60 | 4355 | | | | | | |
| Reference 51 | | 3.49 | 5736 | | | | 88 | 0.37 | | |

^aDensity functional theory.^bSecond-order Møller-Plesset perturbation theory.

excellent approximations to the potentials at the CBS limits.

The long-range Ba-RG interactions deserve special consideration. First, the fitted C_6 coefficients do not follow a regular trend for the RG, even with basis set saturation and even though there are regular changes in the well depths. Moreover, reasonable accuracy for C_6 is readily achieved with the smallest CTZ set. This indicates that the higher-order dispersion components are responsible for a gradual increase of interaction strength with the basis set saturation; this is often called incipient chemical bonding. Second, in all the cases, the fitted C_6 values are smaller by 1%-2% than the values computed through Eq. (3) with the CCSD(3) polarization propagator technique. Note that long-range fits normally tend to overestimate the lowest-order coefficient due to contamination by higher-order contributions, whereas polarization propagator calculations underestimate $\alpha_D(0)$ for Ba (see Table I). This

underestimation cannot be compensated by small underestimates of the RG static polarizabilities: scaling the asymptotic C_6 coefficients from the finite-field calculations of the $\alpha_D(0)$ for Ba and the RGs always increases its value further. It is concluded that the CCSD(3) polarization propagator does not perfectly reproduce the dynamic dipole polarizabilities as a function of imaginary frequency.

Comparison with the literature data^{47-49,51} reveals significant and non-systematic disagreement. In each of these studies, two-electron Ba pseudopotentials were used with reference to the Ba²⁺-RG interactions. As will be shown below, those values do not match the dication potentials calculated here or those calculated by McGuirk *et al.*⁵⁰ Another source of error in those calculations is the description of the interaction between the outer electrons of Ba and RG atoms. For instance, explicit correlation treatment of the 8 outer Xe electrons⁴⁹ better matches the accurate values for Ba-Xe than does representation of Xe

by a pseudopotential.⁵¹ Davis and McCaffrey⁴ used the ECP CCSD(T) technique with an aug-cc-pVQZ basis set, similar to ours, but carried out more extensive correlation treatment of the core electrons of the RG atoms. Quite reasonably, their results fall between the present aug-cc-pwCVTZ and aug-cc-pwCVQZ ones, being closer to the latter. Their deviation from the present ECP/CBS potentials exceeds 2% for R_e and 10% for D_e values.

The cation interaction potentials are summarized in Table IV. All the parameters vary systematically toward the CBS limit and are well reproduced in the C5Z/BF calculations. In contrast to the C_6 for the neutral, C_4 exhibits regular behavior. This reflects a slight increase of $\alpha_D^{\text{RG}}(0)$ with saturation of the basis set. Most of the fitted coefficients slightly exceed their asymptotic counterparts, likely because of the higher-order contaminants mentioned above.

In their CCSD(T) calculations, McGuirk and co-workers⁵⁰ used the same Ba ECP that we used, but with a specially constructed basis set claimed to be similar to the standard aug-cc-pV5Z one. In fact, their results are closer to our CQZ results, which simply reflects better efficiency of the core-valence correlation-consistent sets for recovering the correlation of the sub-valence Ba electrons. For the RG atoms, they also used the same ECP descriptions as here, but with the aug-cc-pV5Z basis set. As the saturation of RG basis set component becomes relatively more important for cations containing heavier rare gases, the quality of the potentials from Ref. 50 gradually increases from “worse than” to “better than” CQZ as one moves from He to Xe. In the same paper, best CCSD(T) R_e , D_e , and ω_e values from CCSD(T) for Ba⁺-Ar were estimated by employing larger basis sets for Ba and Ar (aug-cc-pwCV5Z) and correlating electrons in the $2s^22p^6$ Ar shells. The results are close to the present C5Z and C5Z/SC (see Table II), but still underestimate the interaction strength with respect to the CBS limit.

Overall, the present CBS potentials improve the previous benchmarks potentials⁵⁰ by 0.5%-1.5% for the bond length and 3%-9% for the well depth. Density functional theory calculation for Ba⁺-Ar⁴¹ greatly underestimates the well depth. By contrast, the pseudopotential approach⁵¹ overestimates it for Ba⁺-Xe, though to a lesser extent than for neutral Ba-Xe.

Our Ba⁺-Ar CBS potential perfectly reproduces the B_0 value determined from a rotationally resolved, cold jet excitation spectrum¹⁸ in a direct way. Vibrational constants, both lower than predicted here, were determined therein using the Morse potential model which, as the authors mentioned, is not accurate enough. Combination of an electrostatic potential model and the Rydberg-Klein-Rees method estimated the D_e value to be 680 cm⁻¹. McGuirk and co-workers⁵⁰ regarded their results as a valuable demonstration of severe deviation of Morse-like behavior and confirmation of the approach used in Ref. 18. The present calculations, however, further depart from the semiempirical spectroscopic model, with the binding energy being closer to the estimate obtained by one of us from inversion of transport data.⁴⁵

Table V provides the parameters of the Ba²⁺-RG potentials. Approaching the CBS limits, the spectroscopic parameters vary in the same way as the equilibrium ones (see above). In contrast to the singly charged cation case, the fitted C_4 values

regularly underestimate the asymptotic values. Comparison with the potentials of McGuirk and co-workers⁵⁰ places them approximately between the CQZ and C5Z levels of the present calculations. Their deviations from the CBS limit are smaller than that for Ba⁺-RG systems, e.g., 0.4%-0.6% for the bond length and 2%-4% for the well depth.

The pseudopotential results by Czuchaj and co-workers^{47,49} deviate significantly from the present potentials, giving too weak a dependence of the interaction strength on the nature of the RG atom. Indeed, the binding energy is overestimated by almost 50% for Ba²⁺-He and underestimated by 30% for Ba²⁺-Xe. This inaccuracy of the pseudopotential description of the “core” Ba²⁺-RG system is likely propagated to the results for the neutral species (see above). Interestingly, other pseudopotential calculations⁵¹ underestimate the Ba²⁺-Xe interaction strength, in contrast to Ba⁺-Xe and, especially, Ba-Xe. This implies that the problems originate not only from the inaccuracy of the core but also from the one- and two-electron treatments of Ba cations and neutrals. Density functional theory and second-order Møller-Plesset calculations⁴¹ underestimate the well depth of Ba⁺-Ar by 20% and 7%, respectively.

III. TRANSPORT CROSS SECTIONS AND ATOMIC DIFFUSION

Collision-dominated experiments involving atoms are described in terms of transport cross sections^{95,96} that depend upon the relative kinetic energy, ϵ . The simplest of these is $Q^{(1)}(\epsilon)$, the momentum-transfer cross section, and it has the largest effect on the diffusion of trace amounts of an atom or ion through a dilute gas. It also dominates the gaseous ion transport coefficients discussed in Sec. IV. Hence, we have made careful calculations of $Q^{(1)}$ for the Ba^{*n*+} species in the RGs, using the ECP/CBS potentials described above.

Figure 3 compares the $Q^{(1)}$ values for Ba in He and in Xe that we have calculated classically with an accuracy of 0.04% using program PC⁹⁷ with those obtained quantum-mechanically with roughly the same accuracy. At low energies, quantum-mechanical effects are noticeable for He gas. However, these energies are much smaller than those of interest in experiments at 100 K or above.

The classical calculations are naturally much faster than the quantum ones. Another advantage is that the accuracy of the integrals in PC is easily controlled by varying the number of quadrature points. Finally, higher-order transport cross sections, $Q^{(l)}$, are generated by PC at the same time as $Q^{(1)}$, whereas each quantum $Q^{(l)}$ has a different expression⁹⁸ in terms of phase shifts.

Figure 3 can be viewed as a test of program PC for neutral systems, equivalent to the extensive tests of ionic systems carried out previously.⁹⁷ Based on these results, we shall hereafter make use only of the classical-mechanical values. Since the accuracy of the interaction potentials used as input to PC is not quantified, when transport cross sections calculated with PC to an accuracy of 0.04%, for example, we shall refer to measurable properties calculated from these cross sections as having a precision of 0.04%.

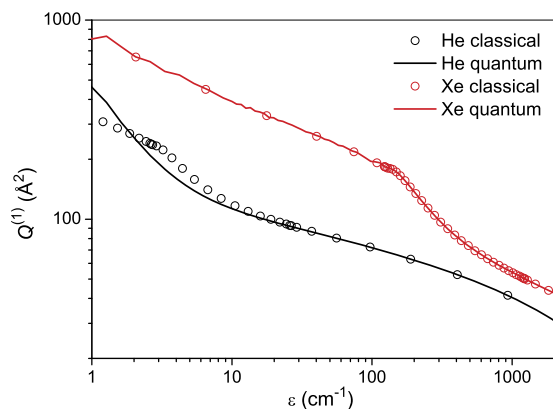


FIG. 3. Classical and quantum-mechanical transport cross sections $Q^{(l)}$ for Ba + He and Ba + Xe collisions as functions of collision energy.

A qualitative way to assess the precision is to examine plots of the microscopic collision frequencies defined as

$$\nu^{(l)}(\epsilon) = \epsilon^{2/m} Q^{(l)}(\epsilon), \quad (4)$$

where $m = 6$ if both particles are neutral and $m = 4$ if one is ionic. Such a plot for $l = 1$ is shown in Fig. 4 for He. At low energies, $\nu^{(1)}(\epsilon)$ is constant, as expected, although at extremely low energies (not shown) the present values become unreliable due to numerical difficulties. The first peaks (at 3 cm^{-1} for Ba, 17 cm^{-1} for Ba^+ , and 450 cm^{-1} for Ba^{2+}) occur at the maximum energies at which classical orbiting can occur for the given potentials. The subsequent minima occur at roughly the energies of the potential minima. The behaviors at higher energies reflect the potentials at small separations. The main point to emphasize, however, is that any other wobbles or extrema shown in such graphs arise from inaccuracies in the interaction potential. We have looked at $\nu^{(1)}(\epsilon)$ for all the Ba^{n+} -RG pairs and have found no evidence of inaccuracies.

The diffusion coefficients of trace amounts of Ba atoms in the RG were measured by Namiotka *et al.*³⁰ Rather than using the traditional method⁹⁵ for calculating these diffusion coefficients from the transport cross sections, we have used program VARY.⁹⁹ In effect, this assumes that a very tiny charge is carried by the neutral atom and that we are only interested in electrostatic fields so weak that they have no influence on this “charged” atom. Then the calculations may be carried out to as high an order of kinetic theory as needed to reach a desired

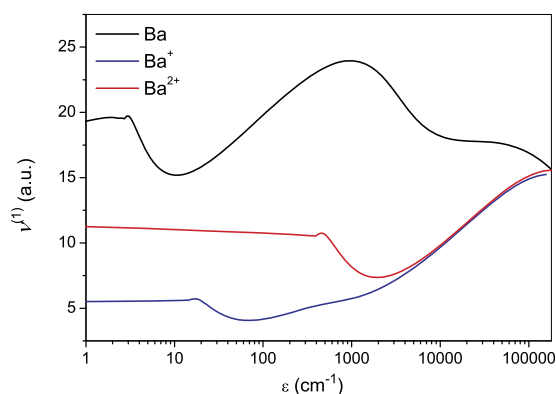


FIG. 4. The frequencies of $\text{Ba}^{n+} + \text{He}$ collisions as a function of collision energy. The $\nu^{(1)}(\epsilon)$ values are given in atomic units ($a_0^2 \sqrt{\text{hartree}}$).

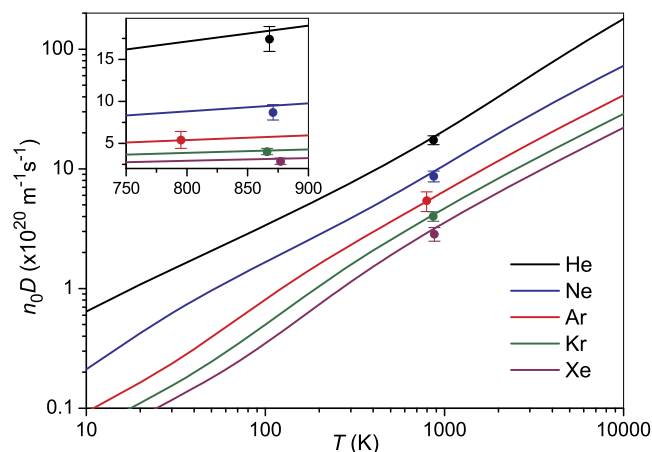


FIG. 5. n_0D , the product of the gas number density and the diffusion coefficient, for Ba atom in RGs, calculated with the ECP/CBS potentials (lines) and derived from the measurements³⁰ (dots), in the double logarithmic scale. The inset emphasizes comparison with the measured data in the linear scale.

fractional accuracy of n_0D , the product of the gas number density and the ion diffusion coefficient. The results for Ba in RGs are shown in Fig. 5 and tabulated in the [supplementary material](#) of this paper. Although the errors in the experimental coefficients are large (on the order of 10%), our potentials clearly give values that agree with them. Calculations within the first-order Enskog-Chapman theory with the Ba–He potential by Czuchaj *et al.*⁴⁷ from Ref. 30 better agree with the medium experimental point. Taking into account large deviations of the pseudopotential results by this group from the present ones, see Table III, it is highly likely that the theoretical diffusion coefficients are more trustworthy than the experimental ones.

We note that there are two advantages in considering n_0D rather than the standard diffusion coefficients reported previously.³⁰ First, it is easy to compare neutral and charged. Second, the equation used to compute the standard diffusion coefficients involves the three-halves power of the ratio of the standard temperature (273.15 K) to the experimental temperature (which range from 795 to 877 K). This strong dependence upon the temperature ratio can produce large variations if the experimental temperature is not well known and well controlled.

IV. GASEOUS ION TRANSPORT

We have used the present potentials as input to program PC⁹⁷ to determine, by classical mechanics, the first 30 transport cross sections. The precisions were between 0.03% and 0.06%, depending upon the specific ion-atom combination being studied. We then used program GC¹⁰⁰ to calculate the ion mobility, the ion temperatures (average kinetic energies) parallel and perpendicular to the electrostatic field, the parallel and perpendicular ion diffusion coefficients, and five other parameters describing the ion velocity distribution functions for Ba cations in the RGs. These calculations were made as functions of E/n_0 at gas temperatures of 100, 200, 300, 400, and 500 K; for He we also used 4.35 K, while for Ba^+ in He and Ar we also used 305 K and 313 K. At low E/n_0 , the precision of the transport coefficients is the same as the precision of the

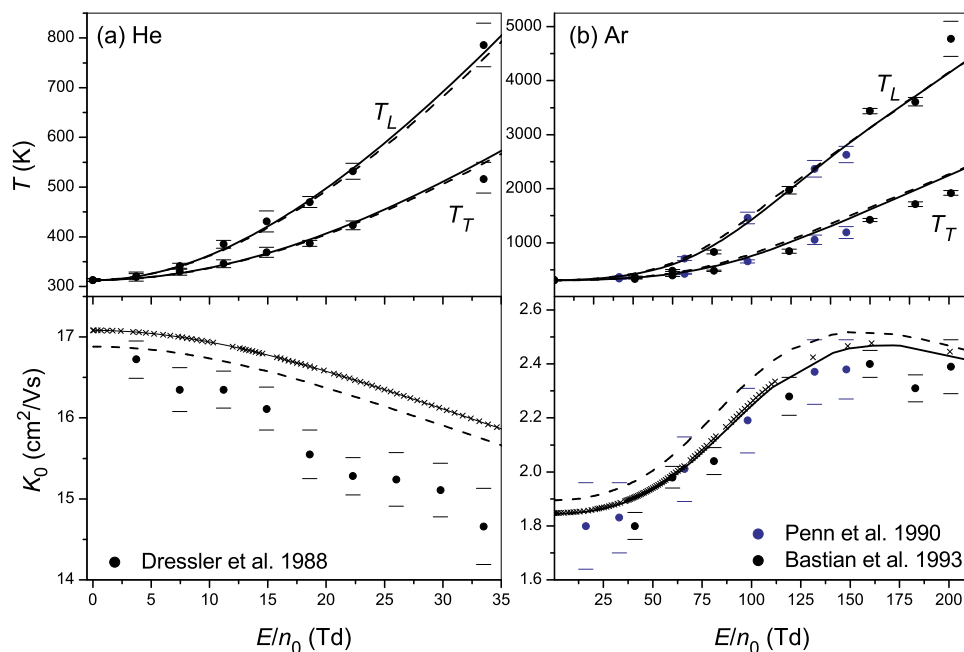


FIG. 6. Comparison of the theoretical and experimental data on Ba^+ transport in (a) He at 313 K and (b) Ar at 305 K. Upper panels: Longitudinal and transverse temperatures of the drifting ion T_L and T_T ; lower panels: mobilities. Theoretical data are represented by solid lines for ECP/CBS potentials, dashed lines for Ref. 50, and crosses for ECP/C5Z/BF potentials (mobility only). Experimental data are taken from the studies of Dressler *et al.*,³⁴ Penn *et al.*,³⁵ and Bastian *et al.*³⁶

transport cross sections; at higher E/n_0 , convergence difficulties led to decreased precision, but this was never worse than 2% for the ion mobilities. In addition, the calculations were repeated for each isotope that occurs naturally for the cations; the gas was always assumed to be the naturally occurring mixture. Approximately 400 tables of results will be added to the on-line database⁵⁴ after this paper is published. Here we only discuss selected results.

For He and Ar buffer gases, the longitudinal (parallel) and transverse (perpendicular) temperatures of the drifting Ba^+ ion, T_L and T_T , were determined by the Leone group^{34–36} from the Doppler shifts of atomic transitions, while the mobilities were deduced from the ion drift times. Indirect pressure measurements were used to determine the E/n_0 dependences. Unfortunately, previous ion-transport calculations⁵⁰ did not agree fully with the measurements by the Leone group.^{34–36} Therefore, we have examined the same properties by using

the ECP/CBS and ECP/C5Z/BF potentials. The upper panels in Fig. 6 show that the ion temperatures are in very close agreement for the three potential-energy functions, although this is somewhat better for He than for Ar. It can be concluded that the present potentials provide better agreement than those in Ref. 50, although this is quite modest: up to 1% for He (35 Td) and up to 4% for Ar (100 Td).

The agreement with the measured mobility values (lower panels in Fig. 6) is quite different. What we believe is that the improvement of the potential for Ba^+ –He induces further departure from experiment, while for Ar the agreement is almost within the experimental error bars. We conclude that the indirectly measured ion mobilities in He are less trustworthy than the other experimental results. In addition, as was noted by McGuirk *et al.*,⁵⁰ systematic uncertainty due to pressure calibration in the experiments cannot be ruled out. We therefore believe that present theoretical results are

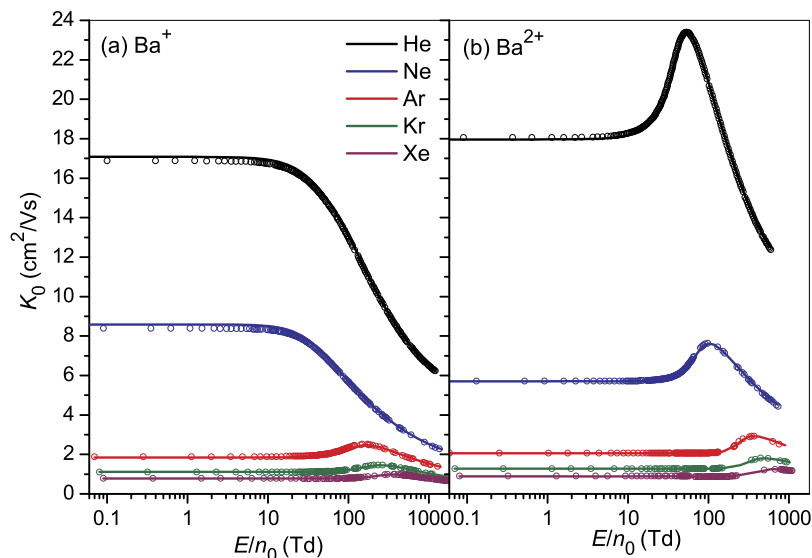


FIG. 7. Mobilities of (a) Ba^+ and (b) Ba^{2+} in rare gases, as computed in Ref. 50 (circles) and in this work with the ECP/CBS potentials (lines). The temperature is 300 K, except 313 K for Ba^+ in He and 305 K Ba^+ in Ar.

accurate enough to be used in place of existing experimental data.

Figure 7 presents the room-temperature mobilities of Ba^+ [panel (a)] and Ba^{2+} [panel (b)] in all rare gases, as computed with the present ECP/CBS potentials and those in Ref. 50. The two sets agree very well: the scale of the figure allows one to catch only slight deviations at very low E/n_0 , which result from minor discrepancies in the C_4 long-range coefficients from the CBS limit (see Tables IV and V). In fact, the overall deviations between two sets do not exceed 4% for Ba^+ [worst case of Ar gas, depicted also in panel (b) of Fig. 6] and 1% for Ba^{2+} . Results obtained with the ECP/C5Z/BF potentials are practically indistinguishable from those from the ECP/CBS calculations, as exemplified in Fig. 6 for Ba^+ in He and Ar.

V. CONCLUDING REMARKS

A consistent set of *ab initio* CCSD(T) potentials for $\text{Ba}^{0,+2+}$ interacting with RG atoms from He to Xe is presented. Using the optimized 46-electron effective core potential ECP46MDF⁵² and augmented correlation-consistent polarized core-valence aug-cc-pwCVnZ (CnZ) basis sets, $n = Q, T, 5$,⁵³ we performed extrapolation to the complete basis set limit and analyzed various factors affecting the accuracy of the potentials near the equilibrium and at long range.

Staying at the CCSD(T) level of correlation treatment, we conservatively estimate the inaccuracy of our interaction energies due to omission of core correlation for RG atoms as 4%. Comparison with all-electron calculations gives an extra 2% for correlation of inner Ba electrons not accounted for in the Dirac-Fock effective core potential. We also admit an inconsistency arising from neglecting the scalar relativistic effects in our description of He, Ne, and Ar, but it is unlikely to exceed 2%. Adding the same amount for ambiguities of the CBS extrapolation and interpolation of the potential curves, we end up with the 10% uncertainty estimate, very conservative and applicable for the whole set of the potentials. For each individual potential, the conservative estimate should be half this size. Of course, taking full account of the triples (and higher-order contributions) in the cluster expansion may well lead to even greater inaccuracies. From the more practical perspective, the potentials reported here are 4%-12% more accurate than the best previously available, from Ref. 4 for neutral Ba and from Ref. 50 for cations. We also advocate here the use of extensive set of bond functions, which brings quintuple-zeta calculations almost to the CBS limit, regardless of the charge state of Ba and the nature of RG atom. Detailed comparison of the neutral and ion transport in dilute rare gases signals a limited sensitivity of the transport properties to interaction potentials. For instance, the relative deviations of the ion mobilities computed with different potentials are often less than half the relative deviations between two potentials. On the other hand, the difference in the Ba^+ mobilities in Ar computed with the previous⁵⁰ and present (ECP/CBS) potentials amounts to 4%, above the usual 2% claimed in ion-mobility spectrometry.¹⁰¹ Unfortunately, experimental data for neutral Ba are too scarce and come with too large uncertainties to serve as the stringent test on the potential accuracy. Although the

calculated diffusion coefficients for Ba in all rare gases fall within the experimental error bars, comparison of Ba^+ mobilities in Ar and especially He indicates that there are systematic deviations. Taking into account the convergence of the calculated transport coefficients with improved potentials and evidences reported in the literature,¹⁰² we recommend for future use the present data available from the database.⁵⁴

SUPPLEMENTARY MATERIAL

See [supplementary material](#) for calculated interaction potentials and Ba atom diffusion coefficients in rare gases.

ACKNOWLEDGMENTS

This work was supported by Russian Science Foundation (Project No. 17-13-01466).

- ¹M. Auger *et al.* (EXO Collaboration), *Phys. Rev. Lett.* **109**, 032505 (2012).
- ²B. Mong *et al.* (nEXO Collaboration), *Phys. Rev. A* **91**, 022505 (2015).
- ³C. Balling and J. J. Wright, *J. Chem. Phys.* **83**, 2614 (1985).
- ⁴B. M. Davis and J. C. McCaffrey, *J. Chem. Phys.* **144**, 044308 (2016).
- ⁵J. Visticot, P. de Pujo, J.-M. Mestdagh, A. Lallemand, J. Berlande, O. Sublemontier, P. Meynadier, and J. Cuvellieret, *J. Chem. Phys.* **100**, 158 (1994).
- ⁶A. I. Krylov and R. B. Gerber, *J. Chem. Phys.* **104**, 3651 (1996).
- ⁷M. Briant, M.-A. Gaveau, and J.-M. Mestdagh, *J. Chem. Phys.* **133**, 034306 (2010).
- ⁸A. Masson, L. Poisson, M.-A. Gaveau, B. Soep, J.-M. Mestdagh, V. Mazet, and F. Spiegelman, *J. Chem. Phys.* **133**, 054307 (2010).
- ⁹A. Masson, M.-C. Heitz, J.-M. Mestdagh, M.-A. Gaveau, L. Poisson, and F. Spiegelman, *Phys. Rev. Lett.* **113**, 123005 (2014).
- ¹⁰S. I. Kanorsky, M. Arndt, R. Dziewior, A. Weis, and T. W. Hänsch, *Phys. Rev. B* **50**, 6296 (1994).
- ¹¹R. Batulin, P. Moroshkin, D. A. Tayurskii, and K. Kono, *AIP Adv.* **8**, 015328 (2018).
- ¹²J. Kielkopf, *J. Phys. B: At. Mol. Phys.* **11**, 25 (1978).
- ¹³H. Harima, K. Tachibana, and Y. Urano, *J. Phys. B: At. Mol. Phys.* **15**, 3679 (1982).
- ¹⁴W. J. Alford, N. Andersen, K. Burnett, and J. Cooper, *Phys. Rev. A* **30**, 2366 (1984).
- ¹⁵T. Maeyama, H. Ito, H. Chiba, K. Ohmori, K. Ueda, and Y. Sato, *J. Chem. Phys.* **97**, 9492 (1992).
- ¹⁶S. Y. Ni, W. Goetz, H. A. J. Meijer, and N. Andersen, *Z. Phys. D* **38**, 303 (1996).
- ¹⁷A. Kowalski, D. J. Funk, and W. H. Breckenridge, *Chem. Phys. Lett.* **132**, 263 (1986).
- ¹⁸S. I. Panov, J. M. Williamson, and T. A. Miller, *J. Chem. Phys.* **102**, 7359 (1995).
- ¹⁹W. H. Breckenridge and C. N. Merrow, *J. Chem. Phys.* **88**, 2329 (1988).
- ²⁰S. Bililign, J. G. Karup, and W. H. Breckenridge, *J. Phys. Chem.* **99**, 7878 (1995).
- ²¹C. Vadla, K. Niemax, V. Horvatic, and R. Beuc, *Z. Phys. D* **34**, 171 (1995).
- ²²J. Brust and A. C. Gallagher, *Phys. Rev. A* **52**, 2120 (1995).
- ²³J. E. Smedley, S. K. Coulter, E. J. Felton, and K. S. Zomlefer, *J. Phys. Chem. A* **112**, 9526 (2008).
- ²⁴E. Anders and N. Grevesse, *Geochim. Cosmochim. Acta* **53**, 197 (1989).
- ²⁵T. Gehren, in *Reviews in Modern Astronomy. I. Cosmic Chemistry*, edited by G. Clare (Springer, Berlin, 1988), p. 52.
- ²⁶L. I. Antipova, A. A. Boyarchuk, Yu. V. Pakhomov, and V. E. Panchuk, *Astron. Rep.* **48**, 597 (2004).
- ²⁷K. A. Nasyrov and A. M. Shalagin, *Astron. Astrophys.* **268**, 201 (1993).
- ²⁸G. Michaud, G. Alecian, and J. Richer, *Atomic Diffusion in Stars* (Springer, Cham, 2015).
- ²⁹T. G. Walker, K. D. Bonin, and W. Happer, *J. Chem. Phys.* **87**, 660 (1987).
- ³⁰R. K. Namiotka, E. Ehrlacher, J. Sagle, M. Brewer, D. J. Namiotka, A. P. Hickman, A. D. Streater, and J. Huennekens, *Phys. Rev. A* **54**, 449 (1996).
- ³¹G. G. Lister, J. J. Curry, and J. E. Lawler, *Phys. Rev. E* **62**, 5576 (2000).
- ³²F. Sigeneger, K. Rackow, D. Uhrlandt, J. Ehlbeck, and G. Lieder, *J. Phys. D: Appl. Phys.* **43**, 385201 (2010).

- ³³R. A. Dressler, H. Meyer, A. O. Langford, V. M. Bierbaum, and S. R. Leone, *J. Chem. Phys.* **87**, 5578 (1987).
- ³⁴R. A. Dressler, J. P. M. Beijers, H. Meyer, S. M. Penn, V. M. Bierbaum, and S. R. Leone, *J. Chem. Phys.* **89**, 4707 (1988).
- ³⁵S. M. Penn, J. P. M. Beijers, R. A. Dressler, V. M. Bierbaum, and S. R. Leone, *J. Chem. Phys.* **93**, 5118 (1990).
- ³⁶M. J. Bastian, C. P. Lauenstein, V. M. Bierbaum, and S. R. Leone, *J. Chem. Phys.* **98**, 9496 (1993).
- ³⁷M. Green, J. Wodin, R. DeVoe, P. Fierlinger, B. Flatt, G. Gratta, F. LePort, M. Montero Díez, R. Neilson, K. O'Sullivan, A. Pocar, S. Waldman, D. S. Leonard, A. Piepke, C. Hargrove, D. Sinclair, V. Strickland, W. Fairbank, Jr., K. Hall, B. Mong, M. Moe, J. Farine, D. Hallman, C. Virtue, E. Baussan, Y. Martin, D. Schenker, J.-L. Vuilleumier, J.-M. Vuilleumier, P. Weber, M. Breidenbach, R. Conley, C. Hall, J. Hodgson, D. Mackay, A. Odian, C. Y. Prescott, P. C. Rowson, K. Skarpaas, and K. Wamba, *Phys. Rev. A* **76**, 023404 (2007).
- ³⁸M. Foerster, H. Guenther, O. Riediger, J. Wiebe, and G. zu Putlitz, *J. Low Temp. Phys.* **110**, 231 (1998).
- ³⁹S.-C. Jeng, W. M. Fairbank, Jr., and M. Miyajima, *J. Phys. D: Appl. Phys.* **42**, 035302 (2009).
- ⁴⁰G. K. Koyanagi and D. K. Bohme, *J. Phys. Chem. Lett.* **1**, 41 (2010).
- ⁴¹B. Hattendorf, B. Gusmini, L. Dorta, R. S. Houk, and D. Günther, *ChemPhysChem* **17**, 2640 (2016).
- ⁴²K. Abdessalem, H. Habli, H. Ghalla, S. J. Yaghmour, F. Calvo, and B. Oujia, *J. Chem. Phys.* **141**, 154308 (2014).
- ⁴³A. Andrejeva, A. M. Gardner, J. B. Graneek, W. H. Breckenridge, and T. G. Wright, *J. Phys. Chem. A* **119**, 5995 (2015).
- ⁴⁴K. Issa, N. Issaoui, H. Ghalla, S. J. Yaghmour, A. M. Mahros, and B. Oujia, *Mol. Phys.* **114**, 118 (2016).
- ⁴⁵L. A. Viehland and D. S. Hampt, *J. Chem. Phys.* **97**, 4964 (1992).
- ⁴⁶E. Czuchaj, F. Rebentrost, H. Stoll, and H. Preuss, *Chem. Phys.* **177**, 107 (1993).
- ⁴⁷E. Czuchaj, F. Rebentrost, H. Stoll, and H. Preuss, *Chem. Phys.* **196**, 37 (1995).
- ⁴⁸J. Brust and C. H. Greene, *Phys. Rev. A* **56**, 2005 (1997).
- ⁴⁹E. Czuchaj, F. Rebentrost, H. Stoll, and H. Preuss, *Theor. Chem. Acc.* **100**, 117 (1998).
- ⁵⁰M. F. McGuirk, L. A. Viehland, E. P. F. Lee, W. H. Breckenridge, C. D. Withers, A. M. Gardner, R. J. Plowright, and T. G. Wright, *J. Chem. Phys.* **130**, 194305 (2009).
- ⁵¹K. Abdessalem, L. Mejrissi, N. Issaoui, B. Oujia, and F. X. Gadéa, *J. Phys. Chem. A* **117**, 8925 (2013).
- ⁵²I. S. Lim, H. Stoll, and P. Schwerdtfeger, *J. Chem. Phys.* **124**, 034107 (2006).
- ⁵³H. Li, H. Feng, W. Sun, Y. Zhang, Q. Fan, K. A. Peterson, Y. Xie, and H. F. Schaefer III, *Mol. Phys.* **111**, 2292 (2013).
- ⁵⁴See www.lxcat.net for Plasma Data Exchange Project.
- ⁵⁵E. Paul-Kwiek, *Mol. Phys.* **99**, 211 (2001).
- ⁵⁶H.-J. Werner, P. J. Knowles, G. Knizia, F. R. Manby, and M. Schütz, "Molpro: A general-purpose quantum chemistry program package," *Wiley Interdiscip. Rev.: Comput. Mol. Sci.* **2**, 242–253 (2012); H.-J. Werner, P. J. Knowles, G. Knizia, F. R. Manby, M. Schütz *et al.*, molpro, version 2015.1, a package of *ab initio* programs, 2015, see <http://www.molpro.net>.
- ⁵⁷P. J. Knowles, C. Hampel, and H.-J. Werner, *J. Chem. Phys.* **99**, 5219 (1993).
- ⁵⁸S. F. Boys and F. Bernardi, *Mol. Phys.* **19**, 553 (1970).
- ⁵⁹D. E. Woon and T. H. Dunning, Jr., *J. Chem. Phys.* **100**, 2975 (1994).
- ⁶⁰D. E. Woon and T. H. Dunning, Jr., *J. Chem. Phys.* **103**, 4572 (1995).
- ⁶¹K. A. Peterson and T. H. Dunning, Jr., *J. Chem. Phys.* **117**, 10548 (2002).
- ⁶²K. A. Peterson, D. Figgen, E. Goll, H. Stoll, and M. Dolg, *J. Chem. Phys.* **119**, 11113 (2003).
- ⁶³K. A. Peterson and K. E. Yousaf, *J. Chem. Phys.* **133**, 174116 (2010).
- ⁶⁴S. M. Cybulski and R. R. Toczyłowski, *J. Chem. Phys.* **111**, 10520 (1999).
- ⁶⁵O. Roos, V. Veryazov, and P.-O. Widmark, *Theor. Chem. Acc.* **111**, 345 (2003).
- ⁶⁶A. Wolf, M. Reiher, and B. A. Hess, *J. Chem. Phys.* **117**, 9215 (2002).
- ⁶⁷W. A. de Jong, R. J. Harrison, and D. A. Dixon, *J. Chem. Phys.* **114**, 48 (2001).
- ⁶⁸H. D. Cohen and C. C. J. Roothaan, *J. Chem. Phys.* **43**, S34 (1965).
- ⁶⁹J. A. Pople, J. W. McIver, Jr., and N. S. Ostlund, *J. Chem. Phys.* **49**, 2960 (1968).
- ⁷⁰T. Korona and H.-J. Werner, *J. Chem. Phys.* **118**, 3006 (2003).
- ⁷¹T. Korona, M. Przybytek, and B. Jeziorski, *Mol. Phys.* **104**, 2303 (2006).
- ⁷²K. A. Peterson, D. E. Woon, and T. H. Dunning, Jr., *J. Chem. Phys.* **100**, 7410 (1994).
- ⁷³D. Feller and J. A. Sordo, *J. Chem. Phys.* **112**, 5604 (2000).
- ⁷⁴J. M. L. Martin, *Chem. Phys. Lett.* **259**, 679 (1996).
- ⁷⁵J. M. L. Martin and P. R. Taylor, *J. Chem. Phys.* **106**, 8620 (1997).
- ⁷⁶M. P. de Lara-Castells, R. V. Krems, A. A. Buchachenko, G. Delgado-Barrio, and P. Villarreal, *J. Chem. Phys.* **115**, 10438 (2001).
- ⁷⁷See <http://physics.nist.gov/asd> for NIST Atomic Spectra Database, version 5.4.
- ⁷⁸H. L. Schwartz, T. M. Miller, and B. Bederson, *Phys. Rev. A* **10**, 1924 (1974).
- ⁷⁹S. Schäfer, M. Mehring, R. Schäfer, and P. Schwerdtfeger, *Phys. Rev. A* **76**, 052515 (2007).
- ⁸⁰I. S. Lim and P. Schwerdtfeger, *Phys. Rev. A* **70**, 062501 (2004).
- ⁸¹B. K. Sahoo and B. P. Das, *Phys. Rev. A* **77**, 062516 (2008).
- ⁸²S. Chattopadhyay, B. K. Mani, and D. Angom, *Phys. Rev. A* **89**, 022506 (2014).
- ⁸³S. Porsev and A. Derevianko, *J. Exp. Theor. Phys.* **102**, 195 (2006).
- ⁸⁴T. F. Gallagher, R. Kachru, and N. H. Tran, *Phys. Rev. A* **26**, 2611 (1982).
- ⁸⁵E. L. Snow and S. R. Lundeen, *Phys. Rev. A* **76**, 052505 (2007).
- ⁸⁶K. Kaur, B. Arora, and B. K. Sahoo, *Phys. Rev. A* **92**, 032704 (2015).
- ⁸⁷E. Iskrenova-Tchoukova and M. S. Safronova, *Phys. Rev. A* **78**, 012508 (2008).
- ⁸⁸U. I. Safronova, *Phys. Rev. A* **81**, 052506 (2010).
- ⁸⁹E. L. Snow, M. A. Gearba, R. A. Komara, S. R. Lundeen, and W. G. Sturrs, *Phys. Rev. A* **71**, 022510 (2005).
- ⁹⁰B. K. Sahoo and B. P. Das, *Phys. Rev. A* **86**, 022506 (2012).
- ⁹¹P. Fuentealba, L. von Szentpaly, H. Preuss, and H. Stoll, *J. Phys. B: At. Mol. Phys.* **18**, 1287 (1985).
- ⁹²R. R. Jones and T. F. Gallagher, *J. Opt. Soc. Am. B* **6**, 1467 (1989).
- ⁹³I. G. Kaplan, *Intermolecular Interactions: Physical Picture, Computational Methods, and Model Potentials* (Wiley, Chichester, 2006).
- ⁹⁴P. L. Fast, M. L. Sánchez, and D. G. Truhlar, *J. Chem. Phys.* **111**, 2921 (1999).
- ⁹⁵J. O. Hirschfelder, C. F. Curtiss, and R. B. Bird, *Molecular Theory of Gases and Liquids* (Wiley, New York, 1954).
- ⁹⁶S. Chapman and T. G. Cowling, *The Mathematical Theory of Non-Uniform Gases*, 3rd ed. (Cambridge University, New York, 1970).
- ⁹⁷L. A. Viehland and C.-L. Yang, *Mol. Phys.* **113**, 3874 (2015).
- ⁹⁸H. T. Wood, *J. Chem. Phys.* **54**, 977 (1971).
- ⁹⁹L. A. Viehland, *Int. J. Ion Mobility Spectrom.* **15**, 21 (2012).
- ¹⁰⁰D. M. Danailov, L. A. Viehland, R. Johnsen, T. G. Wright, and A. S. Dickinson, *J. Chem. Phys.* **128**, 134302 (2008).
- ¹⁰¹G. A. Eiceman and Z. Karpas, *Ion Mobility Spectrometry* (CRC Press, Boca Raton, Florida, 2005).
- ¹⁰²L. A. Viehland, T. Skaist, C. Adhikari, and W. F. Siems, *Int. J. Ion Mobility Spectrom.* **20**, 1 (2017).